Electronic Supplementary Information

Borohydride stabilized gold-silver bimetallic nanocatalysts for highly efficient 4-nitrophenol reduction

Nathaniel E. Larm, Jason A. Thon, Yahor Vazmitsel, Jerry L. Atwood, and Gary A. Baker*

Experimental Section

Materials. Ultrapure Millipore water purified to a resistivity of 18.2 MΩ cm was used throughout. Tetrachloroauric acid trihydrate ($HAuCl_4 \cdot 3\ H_2O$, ≥99.9%, 520918), silver nitrate ($AgNO_3$, 99.9999%, 204390), sodium borohydride ($NaBH_4$, 99.99%, 480886), and 4-nitrophenol (4-NP, ≥99%, 241326) were all acquired from Millipore Sigma (St. Louis, MO) and used as received.

Characterization. UV–vis spectroscopy was performed using a Cary 50 Bio UV–vis spectrometer with disposable, 1-cm path length poly(methyl methacrylate) (PMMA) cuvettes. Transmission electron microscopy (TEM) images of 5-day-old NPs deposited on carbon-coated copper grids (Ted Pella, Inc.; 01814-F, support films, carbon type-B, 400 mesh) were obtained using an FEI Technai (F20) microscope operating at 200 keV. At least 300 particles were analyzed using ImageJ software to generate NP size histograms.

Nanocatalyst Synthesis. 18.0 mL of ultrapure H_2O was added to each of thirty-three 50-mL polypropylene centrifuge tubes. The appropriate volume of 5.0 mM $HAuCl_4 \cdot 3H_2O$ was added to each tube according to the experimental parameters given in Tables S1–S3. 10.0, 25.0, and 50.0 mM $NaBH_4$ solutions were prepared immediately before use. Two 1000-μL autopipettors were used to rapidly and simultaneously inject the appropriate amounts of 5.0 mM $AgNO_3$ and $NaBH_4$ stock to the $HAuCl_4$ solution under vortex mixing, achieving a BH_4^- to metal molar ratio of 2.0, 5.0, or 10.0 based on the sample set in Tables S1–S3. The resulting solutions, which immediately turned a shade of red to yellow depending on the metal ratio, were vortexed for an additional 20 s to mix. UV–vis absorption spectroscopy was used to follow the colloidal stability of the nanoparticles during aging for 1, 5, 10, 20, and 30 d. All solutions were kept at room temperature and stored protected from light during aging.

Nitroarene Reduction. The catalytic activity for 4-nitrophenol (4-NP) reduction to 4-aminophenol (4-AP) using $NaBH_4$ was assessed for each sample that did not visibly show black aggregates after aging for 5 d. First, 2.1 mL of 0.20 mM 4-NP and 0.9 mL of fresh 0.1 M $NaBH_4$ were combined in a clean 4-mL PMMA cuvette and placed in the UV–vis spectrometer set to scan at 400 nm. To initiate a catalytic run, 0.034 mL of a given nanoparticle solution (0.25 mM metal) was added, followed by rapid capping and inversion of the cuvette to mix before placing it in the spectrometer. The reaction was assumed to have completed when the absorbance at 400 nm was at 5% of the starting value. For a large excess of borohydride ($NaBH_4$:4-NP ratio of 214

was used throughout), the pseudo-first-order kinetics yield a linear plot of $\ln(A_0/A_t)$ *versus* time, where A_0 and A_t are the initial and time-dependent absorbance, respectively, with the slope equaling the apparent rate (k_{app}). All kinetic studies were performed in triplicate.

Evaluation of Economics. At the time of this writing, 1 g of $AgNO_3$ costs $24.70 (99.9999% trace metals basis, 204390) whereas 1 g of $HAuCl_4 \cdot 3H_2O$ runs $127.00 (99.9% trace metals basis, 520918) from Millipore Sigma. Notably, the TOF/USD ratio increased over 85-fold between $x = 1.0$ and $x = 0.1$ for Au_xAg_{1-x} NPs made for R = 5. Error bars were derived from the uncertainty in the TOF and do not account for price variability.

Table S1 R = 2 sample preparation for Au_xAg_{1-x}NPs reduced and stabilized by $NaBH_4$.

Stocks	[stock] (mM)	*x*	Water (mL)	$HAuCl_4$ stock (mL)	Total (mL)	$AgNO_3$ stock (mL)	$NaBH_4$ stock (mL)	Final volume (mL)
$HAuCl_4$	5.0	1.0	18.0	1.0	19.0	0.0	1.0	20.0
$AgNO_3$	5.0	0.9	18.0	0.9	18.9	0.1	1.0	20.0
$NaBH_4$	10.0	0.8	18.0	0.8	18.8	0.2	1.0	20.0
		0.7	18.0	0.7	18.7	0.3	1.0	20.0
		0.6	18.0	0.6	18.6	0.4	1.0	20.0
		0.5	18.0	0.5	18.5	0.5	1.0	20.0
		0.4	18.0	0.4	18.4	0.6	1.0	20.0
		0.3	18.0	0.3	18.3	0.7	1.0	20.0
		0.2	18.0	0.2	18.2	0.8	1.0	20.0
		0.1	18.0	0.1	18.1	0.9	1.0	20.0
		0.0	18.0	0.0	18.0	1.0	1.0	20.0

Table S2 R = 5 sample preparation for Au_xAg_{1-x}NPs reduced and stabilized by $NaBH_4$.

Stocks	[stock] (mM)	*x*	Water (mL)	$HAuCl_4$ stock (mL)	Total (mL)	$AgNO_3$ stock (mL)	$NaBH_4$ stock (mL)	Final volume (mL)
$HAuCl_4$	5.0	1.0	18.0	1.0	19.0	0.0	1.0	20.0
$AgNO_3$	5.0	0.9	18.0	0.9	18.9	0.1	1.0	20.0
$NaBH_4$	25.0	0.8	18.0	0.8	18.8	0.2	1.0	20.0
		0.7	18.0	0.7	18.7	0.3	1.0	20.0
		0.6	18.0	0.6	18.6	0.4	1.0	20.0
		0.5	18.0	0.5	18.5	0.5	1.0	20.0
		0.4	18.0	0.4	18.4	0.6	1.0	20.0
		0.3	18.0	0.3	18.3	0.7	1.0	20.0
		0.2	18.0	0.2	18.2	0.8	1.0	20.0
		0.1	18.0	0.1	18.1	0.9	1.0	20.0
		0.0	18.0	0.0	18.0	1.0	1.0	20.0

Table S3 R = 10 sample preparation for Au_xAg_{1-x}NPs reduced and stabilized by $NaBH_4$.

Stocks	[stock] (mM)	x	Water (mL)	$HAuCl_4$ stock (mL)	Total (mL)	$AgNO_3$ stock (mL)	$NaBH_4$ stock (mL)	Final volume (mL)
$HAuCl_4$	5.0	1.0	18.0	1.0	19.0	0.0	1.0	20.0
$AgNO_3$	5.0	0.9	18.0	0.9	18.9	0.1	1.0	20.0
$NaBH_4$	50.0	0.8	18.0	0.8	18.8	0.2	1.0	20.0
		0.7	18.0	0.7	18.7	0.3	1.0	20.0
		0.6	18.0	0.6	18.6	0.4	1.0	20.0
		0.5	18.0	0.5	18.5	0.5	1.0	20.0
		0.4	18.0	0.4	18.4	0.6	1.0	20.0
		0.3	18.0	0.3	18.3	0.7	1.0	20.0
		0.2	18.0	0.2	18.2	0.8	1.0	20.0
		0.1	18.0	0.1	18.1	0.9	1.0	20.0
		0.0	18.0	0.0	18.0	1.0	1.0	20.0

Table S4 Turnover frequency (TOF/h^{-1}) of Au_xAg_{1-x}NPs.

x	R = 2	R = 5	R = 10
1.0	605 ± 10	620 ± 40	590 ± 10
0.9	2,926 ± 50	1,310 ± 50	2,460 ± 70
0.8	4,010 ± 200	5,400 ± 330	6,500 ± 230
0.7	8,830 ± 480	8,600 ± 170	9,690 ± 1240
0.6	11,500 ± 740	7,980 ± 40	9,160 ± 660
0.5	8,180 ± 50	9,500 ± 240	12,070 ± 1,370
0.4	7,930 ± 1,190	8,840 ± 60	[a]
0.3	12,160 ± 230	10,450 ± 390	[a]
0.2	8,590 ± 1,100	9,600 ± 830	[a]
0.1	8,280 ± 210	9,000 ± 410	[a]
0.0	2,370 ± 70	[a]	[a]

[a] Catalytic activity was not assessed for these samples due to the presence of black precipitate, evidence of NP aggregation.

Table S5 Apparent catalytic rate (k_{app}/s^{-1}) and turnover frequency (TOF/h^{-1}) for the recyclability study performed using the R = 2, x = 0.3 bimetallic Au_xAg_{1-x}NPs.

Cycle	k_{app} (s^{-1})	TOF (h^{-1})
1	1.87×10^{-1}	12,260
2 (1st recycle)	9.77×10^{-2}	6,030
3 (2nd recycle)	7.22×10^{-2}	4,490
4 (3rd recycle)	4.17×10^{-2}	2,880
5 (4th recycle)	3.30×10^{-2}	2,120
6 (5th recycle)	2.68×10^{-2}	1,570

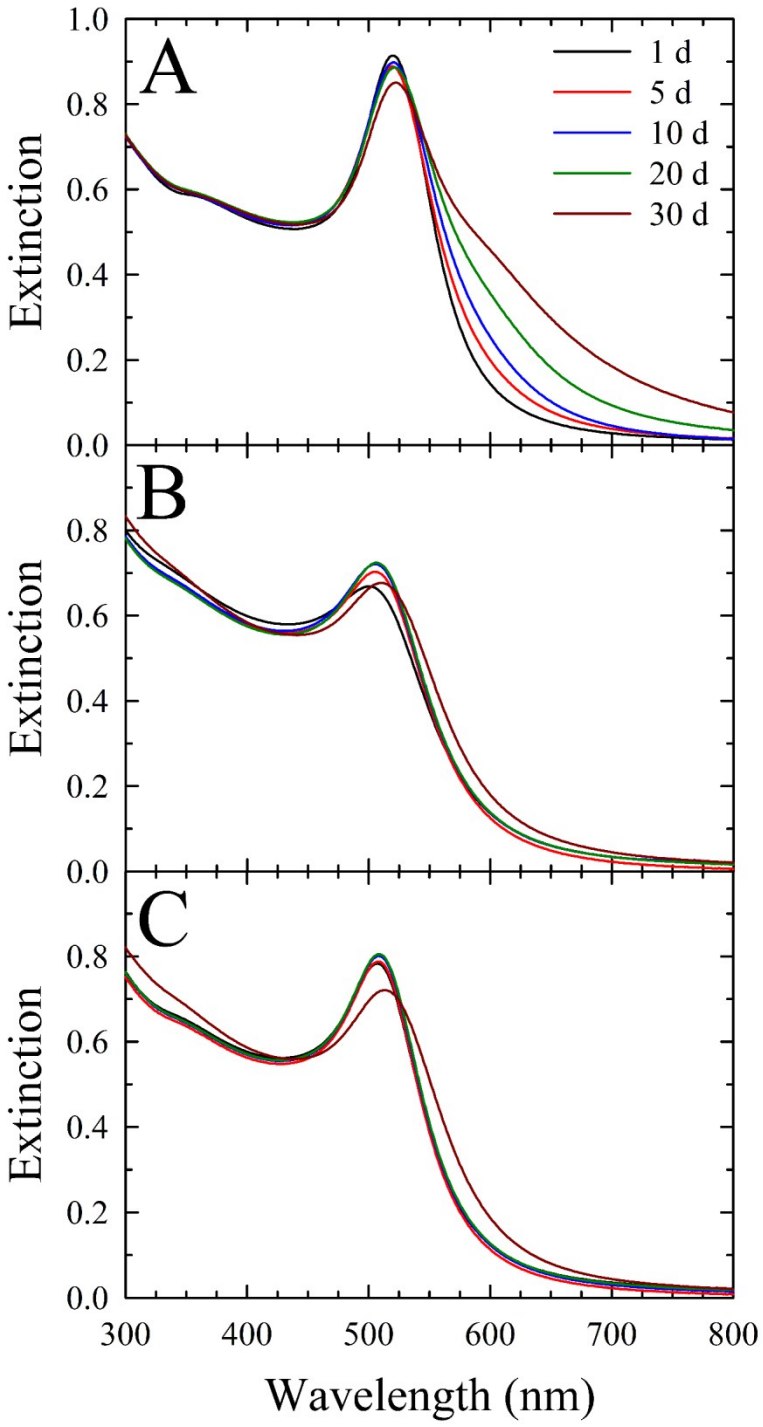

Fig. S1 Stability of AuNPs (Au_xAg_{1-x}NPs for x = 1.0) over 30 days of storage as monitored using UV–vis spectrophotometry. Panels A, B, and C correspond to R values of 2, 5, and 10, respectively. The legend in panel A applies to all panels.

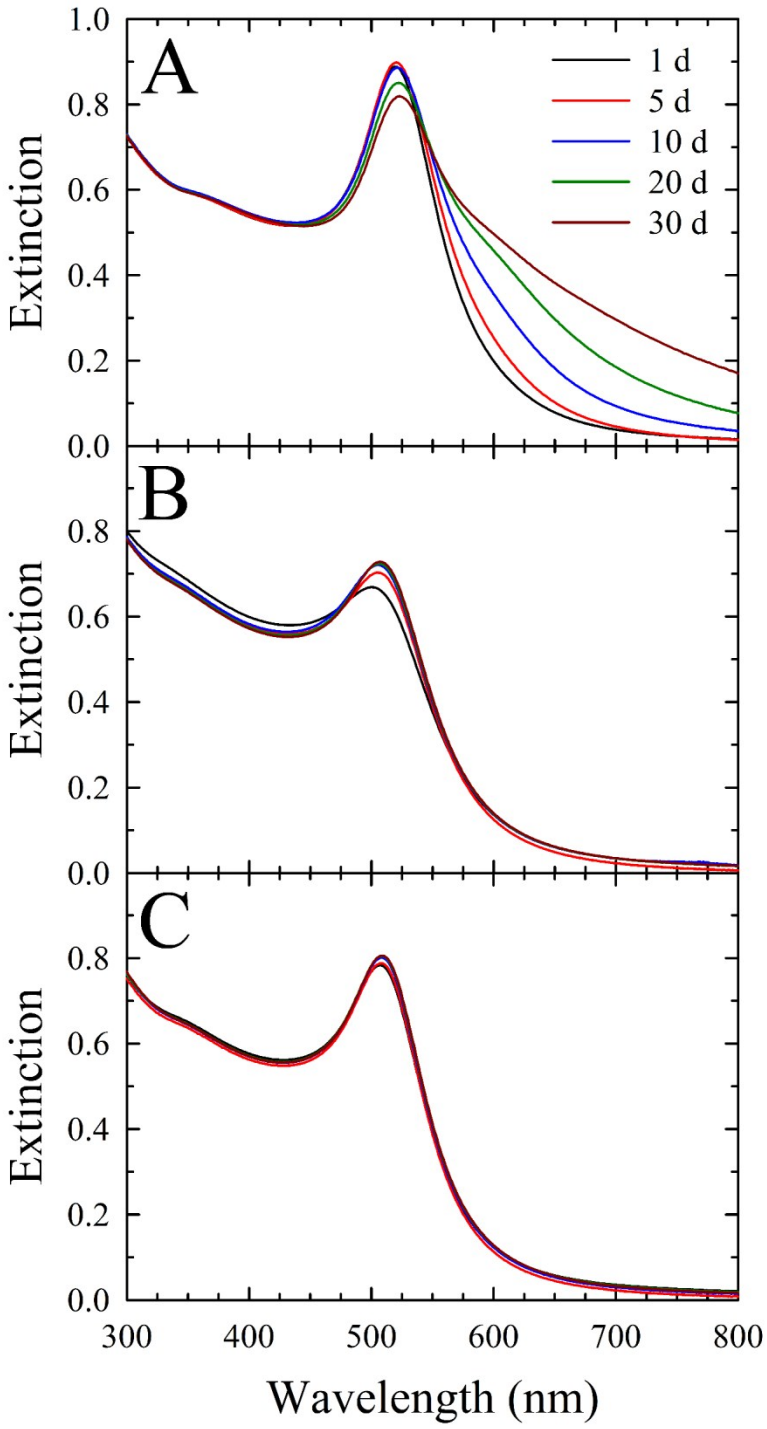

Fig. S2 Stability of Au_xAg_{1-x}NPs (x = 0.9) over 30 days of storage as followed by UV–vis spectrophotometry. Panels A, B, and C correspond to R values of 2, 5, and 10, respectively. The legend in panel A applies to all panels.

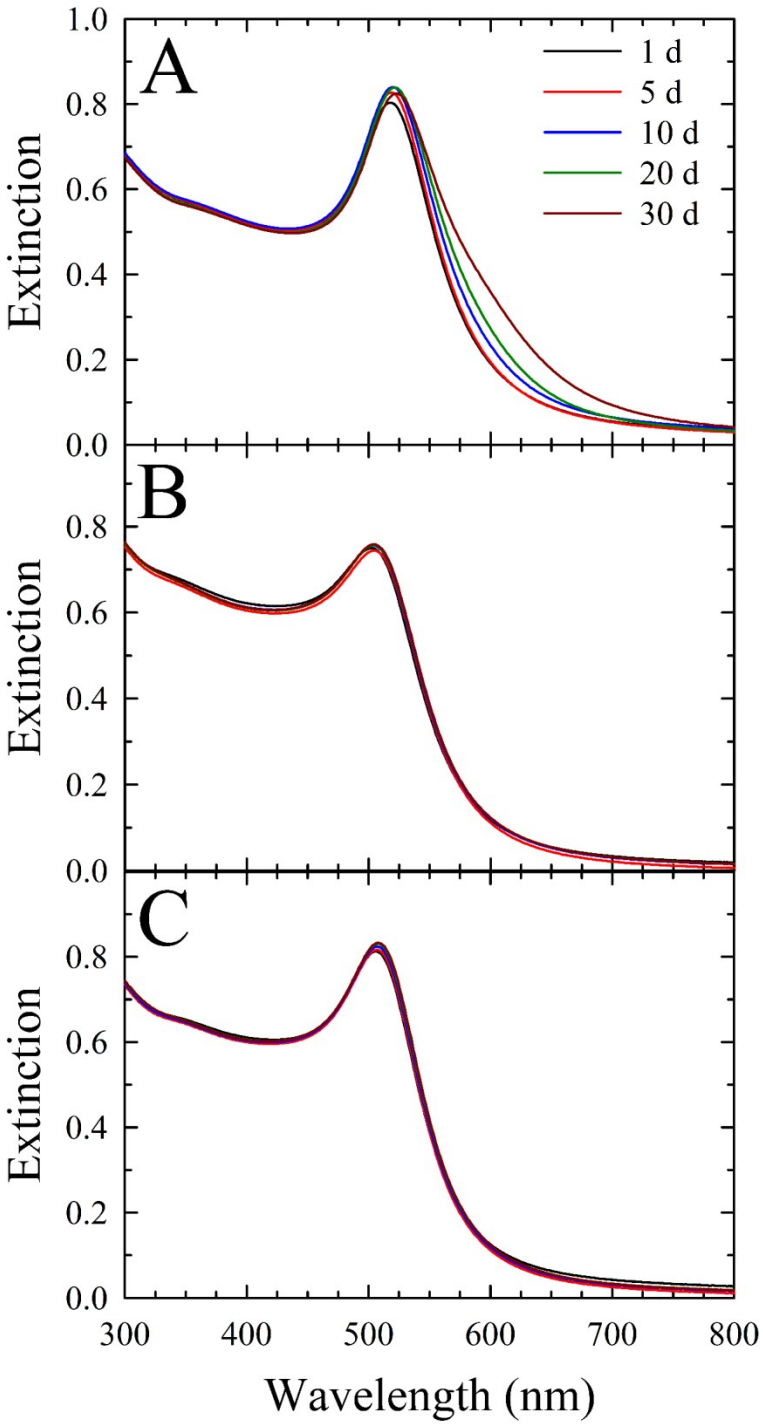

Fig. S3 Stability of Au_xAg_{1-x}NPs (x = 0.8) over 30 days of storage, interrogated using UV–vis spectrophotometry. Panels A, B, and C correspond to R values of 2, 5, and 10, respectively. The legend in panel A applies to all panels.

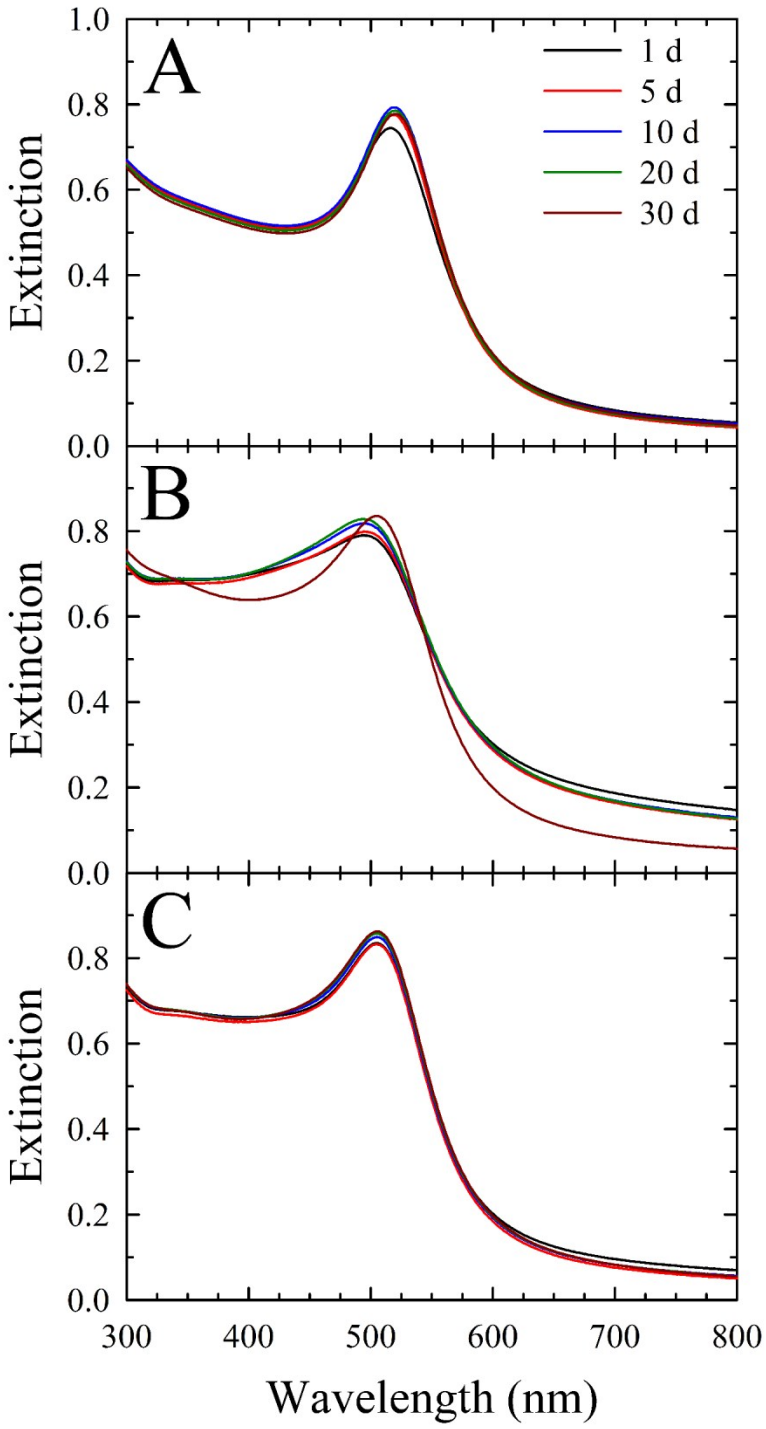

Fig. S4 Stability of Au_xAg_{1-x}NPs (x = 0.7) over 30 days of storage as monitored using UV–vis spectrophotometry. Panels A, B, and C correspond to R values of 2, 5, and 10, respectively. The legend in panel A applies to all panels.

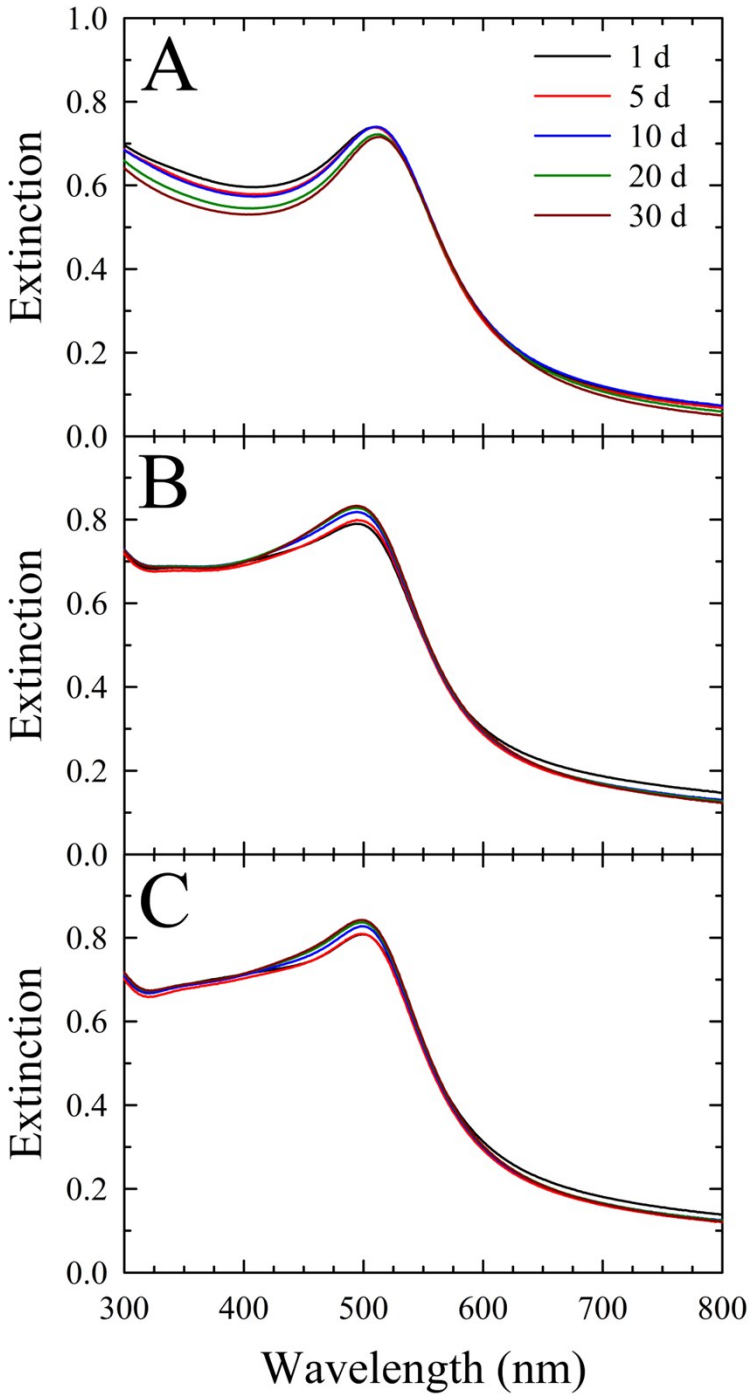

Fig. S5 Stability of Au_xAg_{1-x}NPs (x = 0.6) over 30 days of storage as measured using UV–vis spectrophotometry. Panels A, B, and C correspond to R values of 2, 5, and 10, respectively. The legend in panel A applies to all panels.

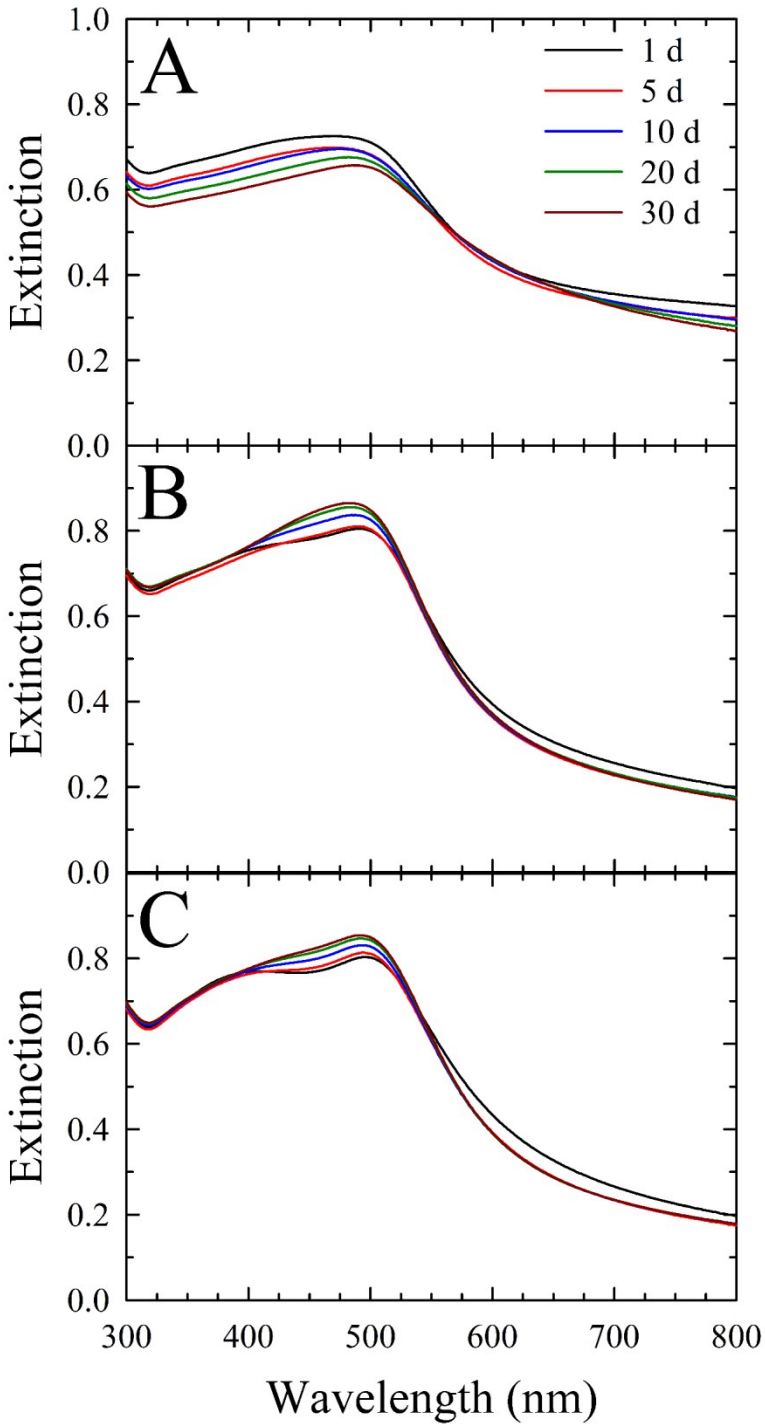

Fig. S6 Stability of Au_xAg_{1-x}NPs (x = 0.5) over 30 days of storage, tracked using UV–vis spectrophotometry. Panels A, B, and C correspond to R values of 2, 5, and 10, respectively. The legend in panel A applies to all panels.

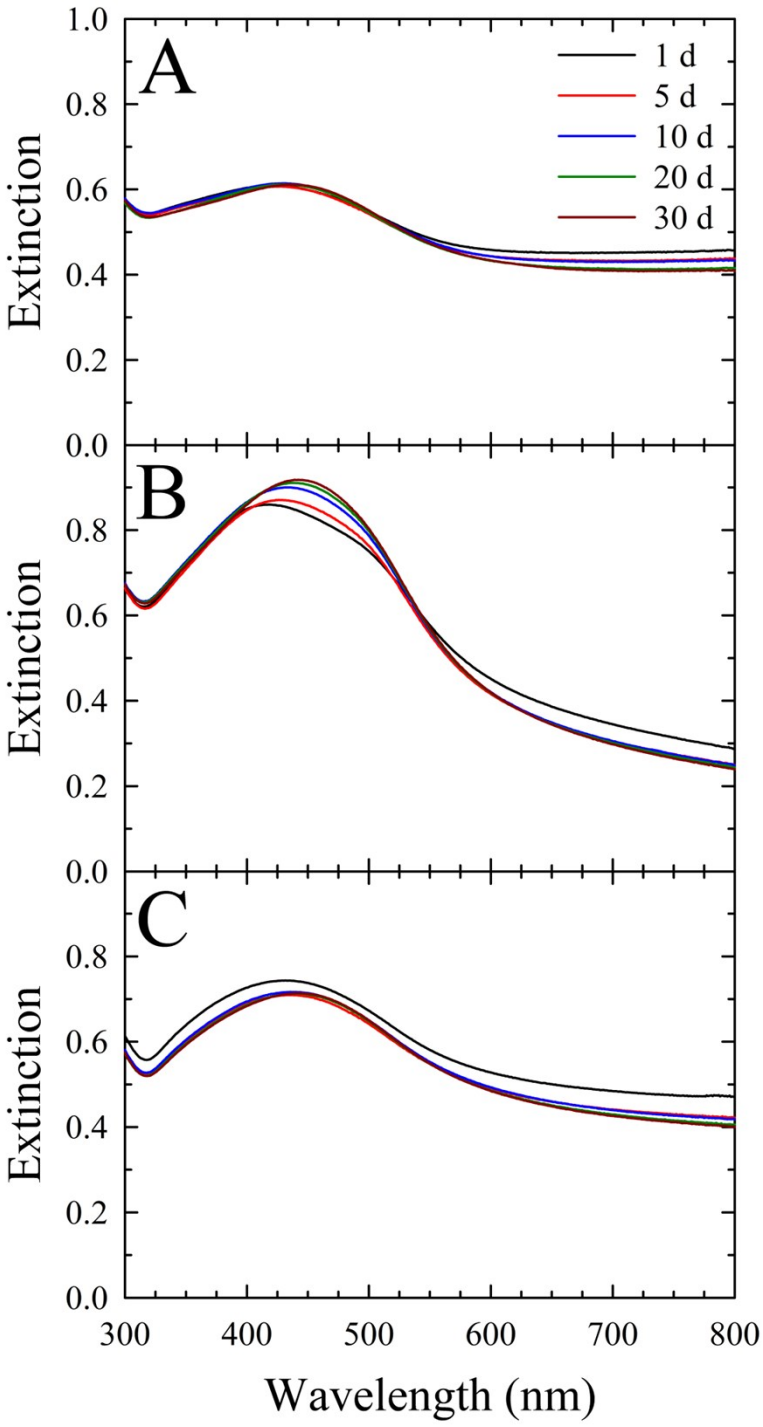

Fig. S7 Stability of Au_xAg_{1-x}NPs (x = 0.4) over 30 days of storage, followed by UV–vis spectrophotometry. Panels A, B, and C correspond to R values of 2, 5, and 10, respectively. The legend in panel A applies to all panels.

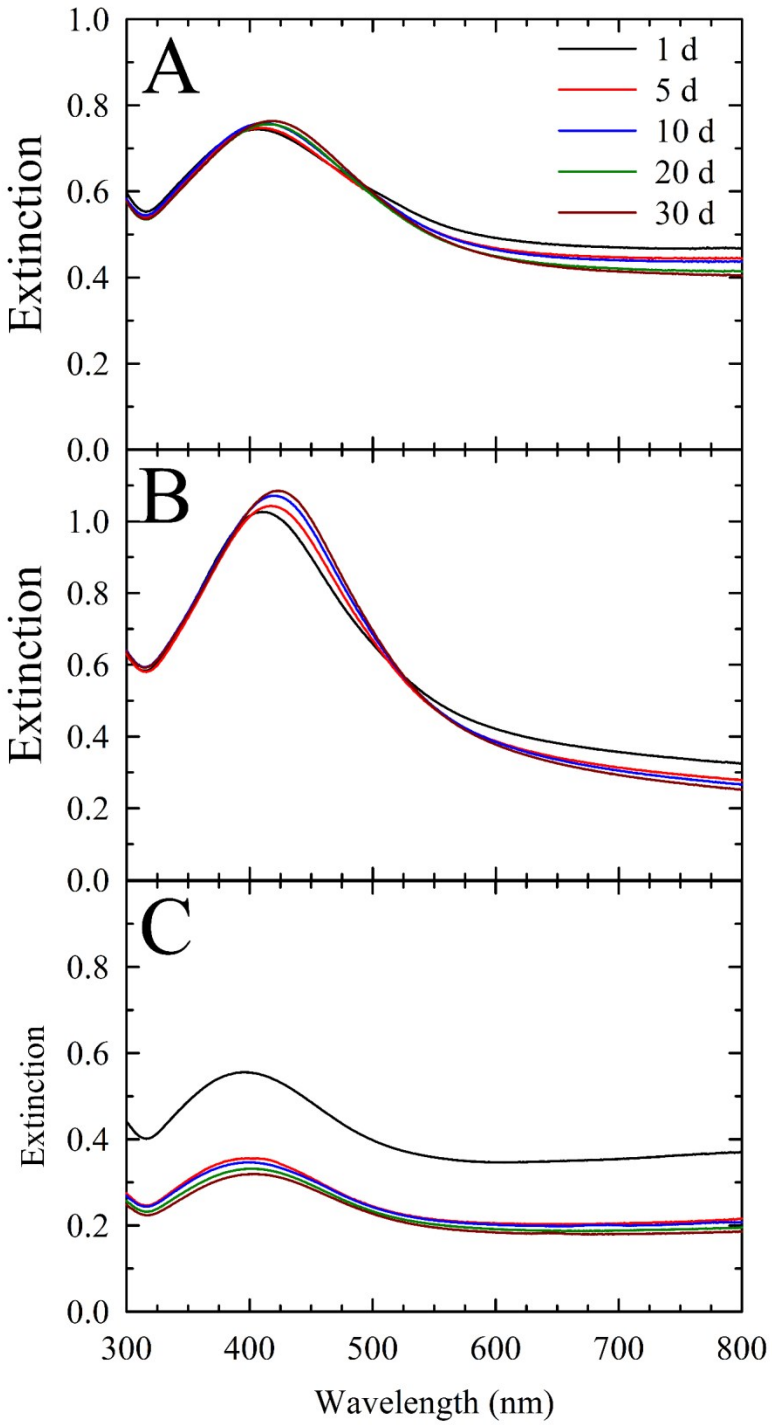

Fig. S8 Stability of Au_xAg_{1-x}NPs (x = 0.3) followed over 30 days of storage using UV–vis spectrophotometry. Panels A, B, and C correspond to R values of 2, 5, and 10, respectively. The legend in panel A applies to all panels.

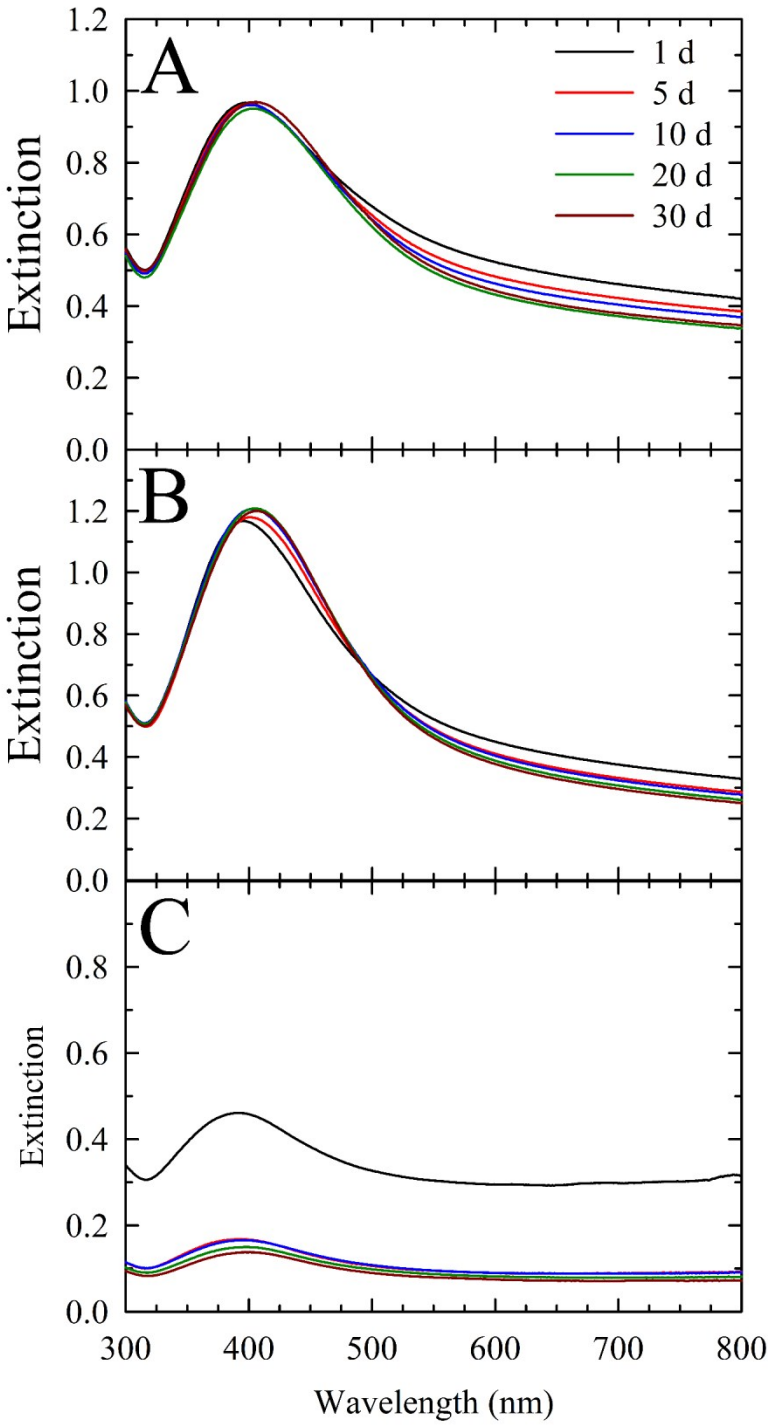

Fig. S9 Stability of Au_xAg_{1-x}NPs (x = 0.2) evaluated over 30 days of storage with UV–vis spectrophotometry. Panels A, B, and C correspond to R values of 2, 5, and 10, respectively. The legend in panel A applies to all panels.

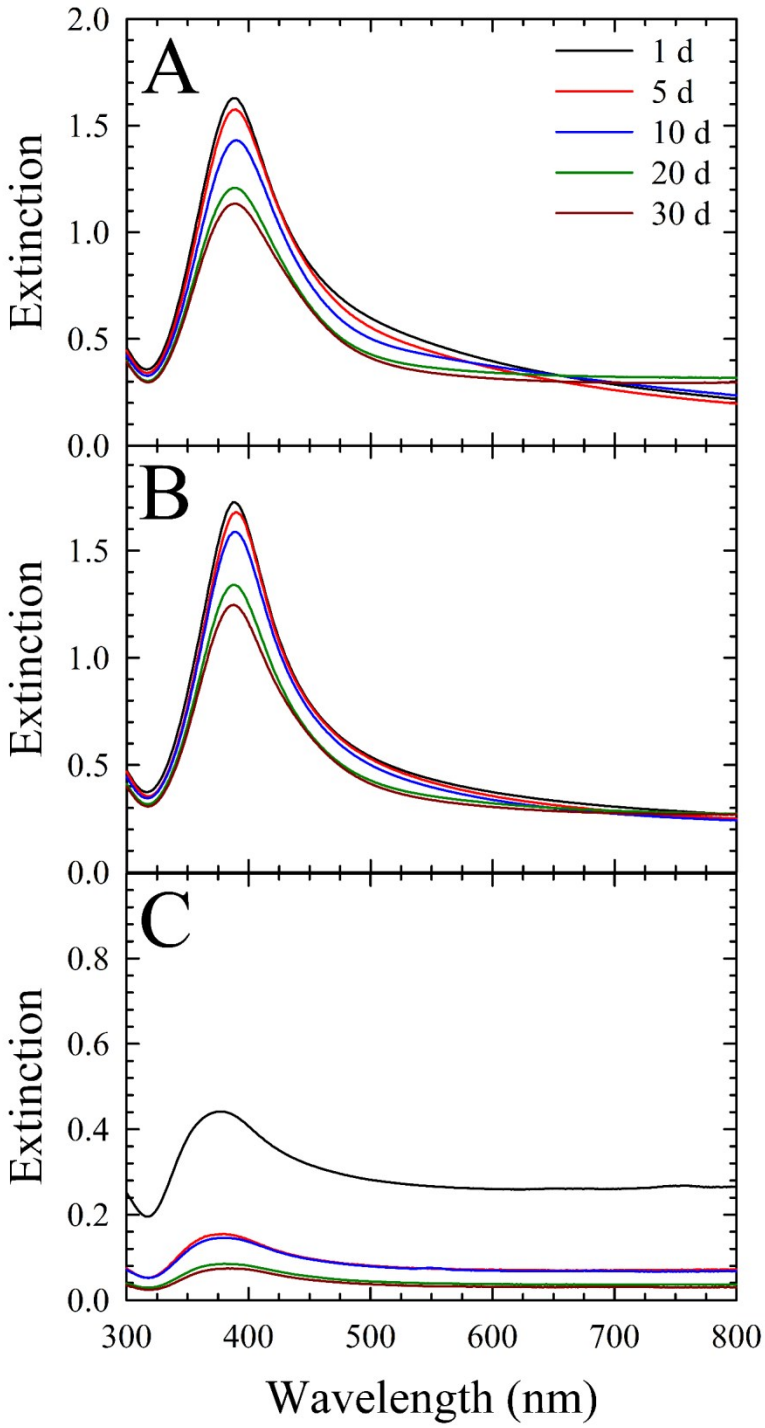

Fig. S10 Stability of Au_xAg_{1-x}NPs (x = 0.1) investigated over 30 days of storage with UV–vis spectrophotometry. Panels A, B, and C correspond to R values of 2, 5, and 10, respectively. The legend in panel A applies to all panels.

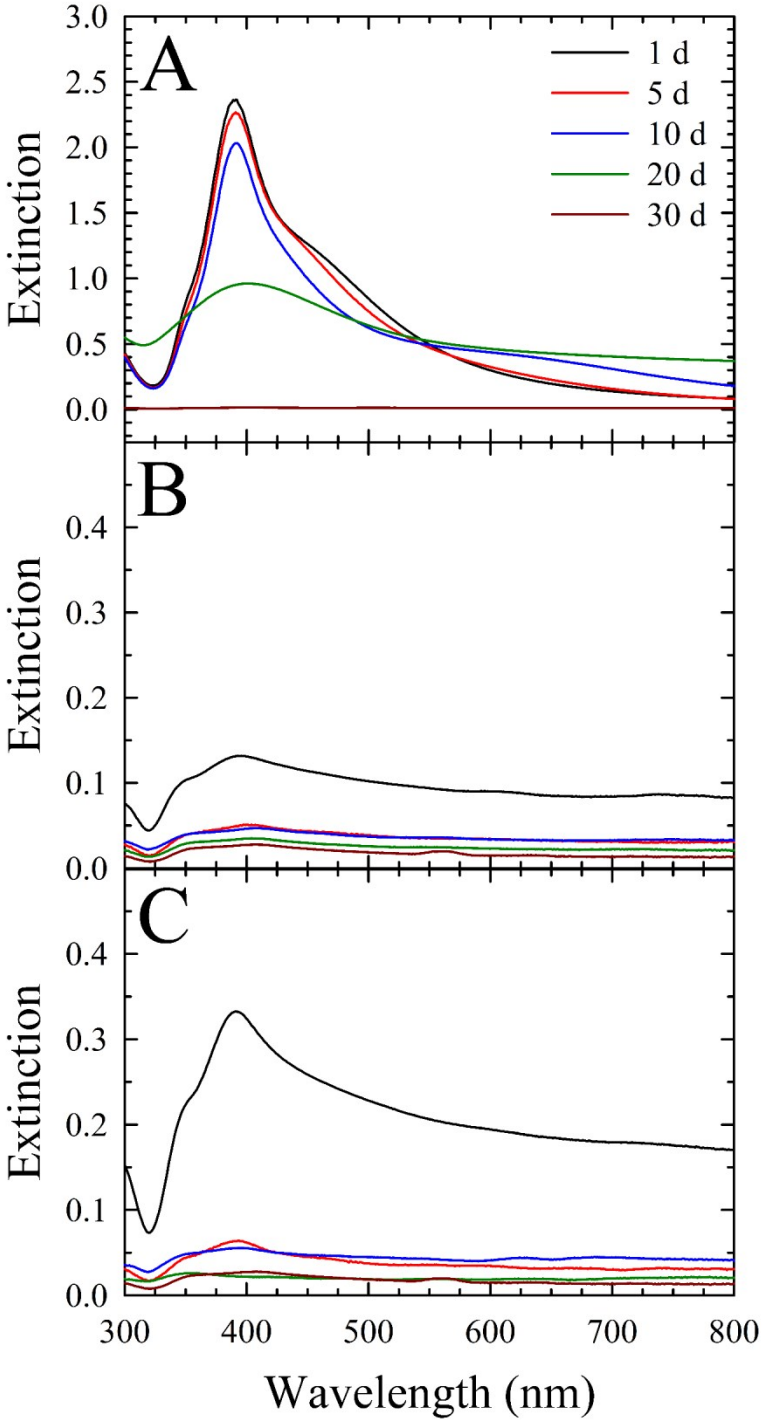

Fig. S11 Stability of AgNPs (Au_xAg_{1-x}NPs for x = 0.0), monitored over 30 days of storage using UV–vis spectrophotometry. Panels A, B, and C correspond to R values of 2, 5, and 10, respectively. The legend in panel A applies to all panels.

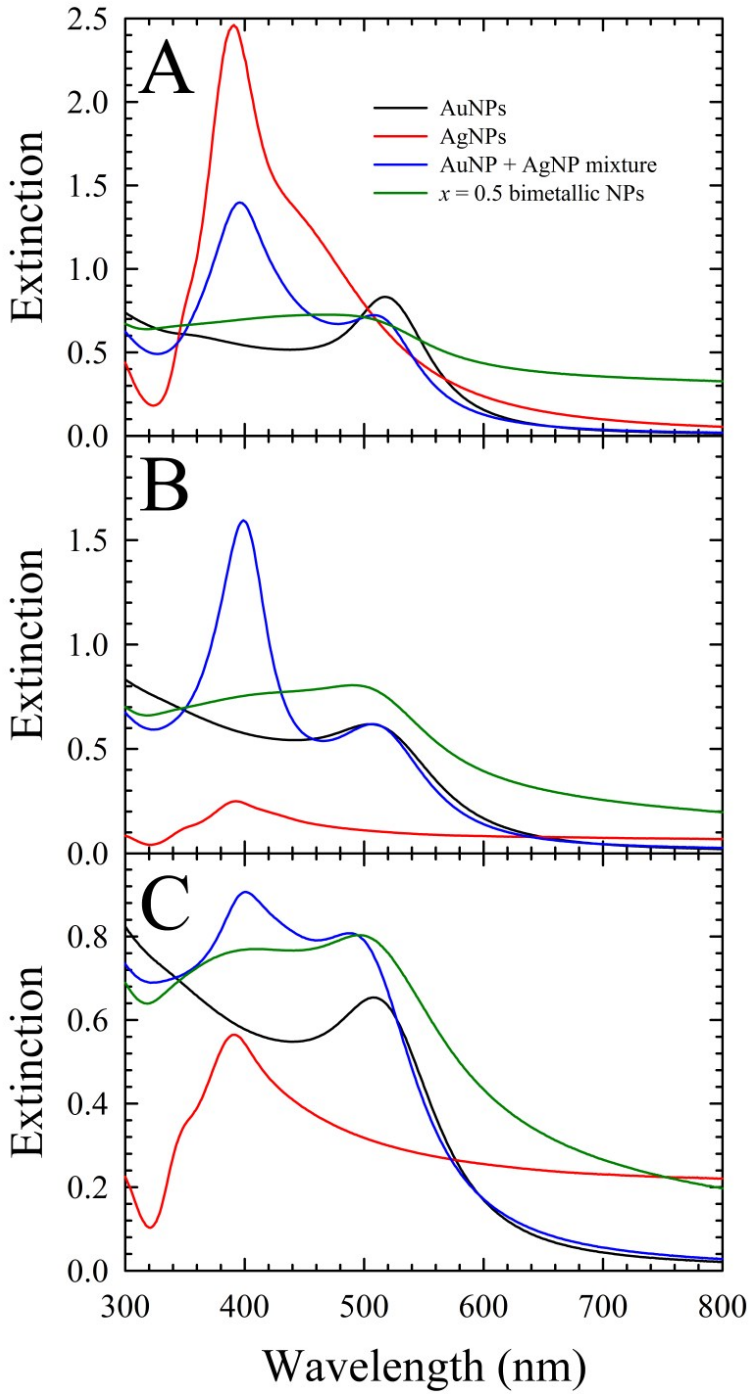

Fig. S12 Comparison of AuNPs, AgNPs, a 1:1 AuNP:AgNP mixture, and bimetallic Au_xAg_{1-x}NPs (x = 0.5). Shown are A) R = 2, B) R = 5, and C) R = 10, where R equals the molar ratio of $NaBH_4$ to metal. The total metal (Au + Ag) concentration is 0.25 mM for all samples.

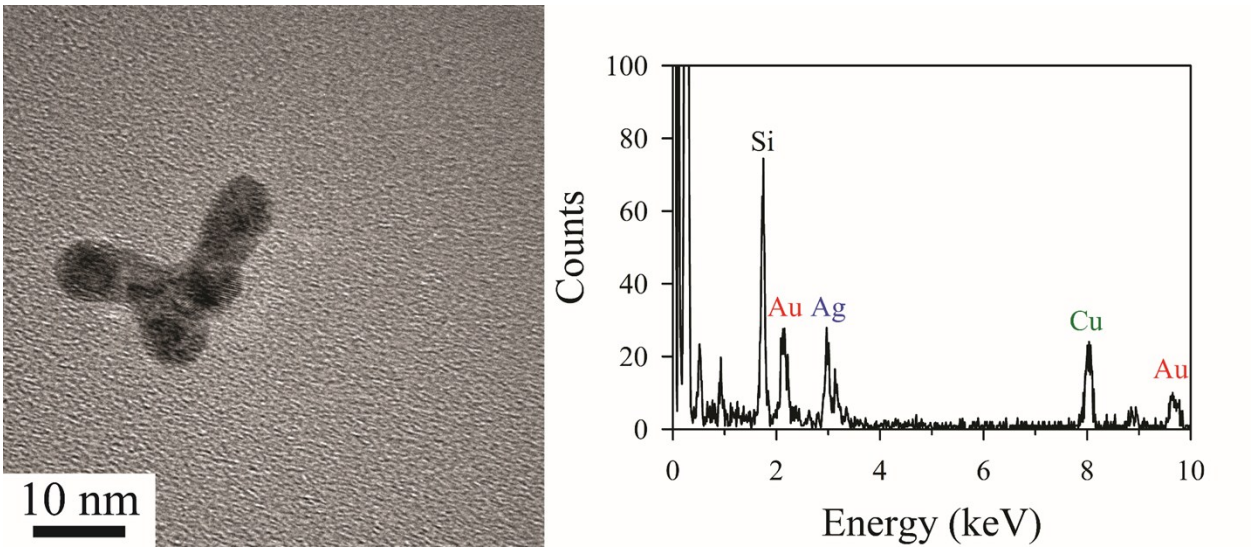

Fig. S13 (Left) A HR-TEM image showing a R = 5, x = 0.5 bimetallic Au_xAg_{1-x}NP and (right) the corresponding EDS spectrum confirming the presence of both gold and silver within the nanostructure. Copper is typically observed when using copper TEM grids, but the presence of silicon is more likely attributed to a small amount of contamination on the TEM grid, as no glassware or silicon-containing reagents were used in the preparation of these bimetallic NPs.

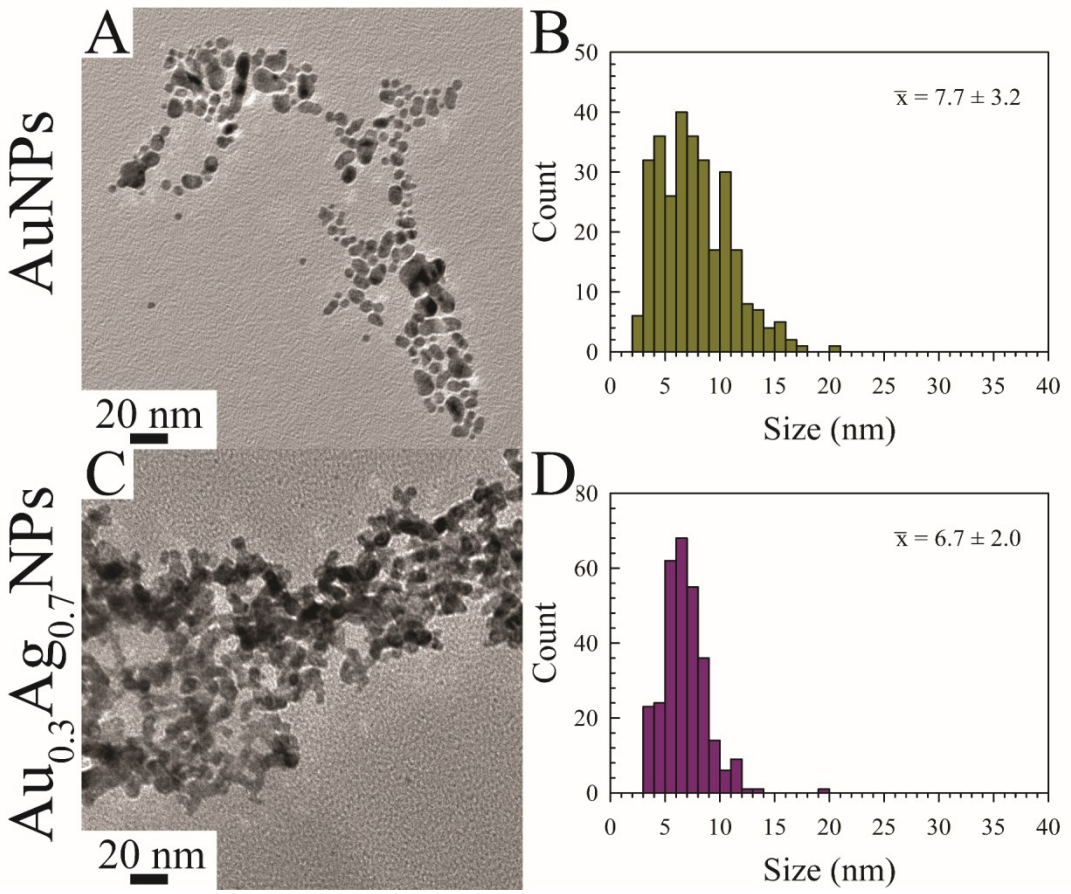

Fig. S14 Representative TEM images and size distribution histograms for R = 5 Au_xAg_{1-x}NPs where (A, B) x = 1.0 and (C, D) x = 0.3. Note the apparent formation of metal networks and particle ripening (sizes of metal networks were ignored during particle size analysis).

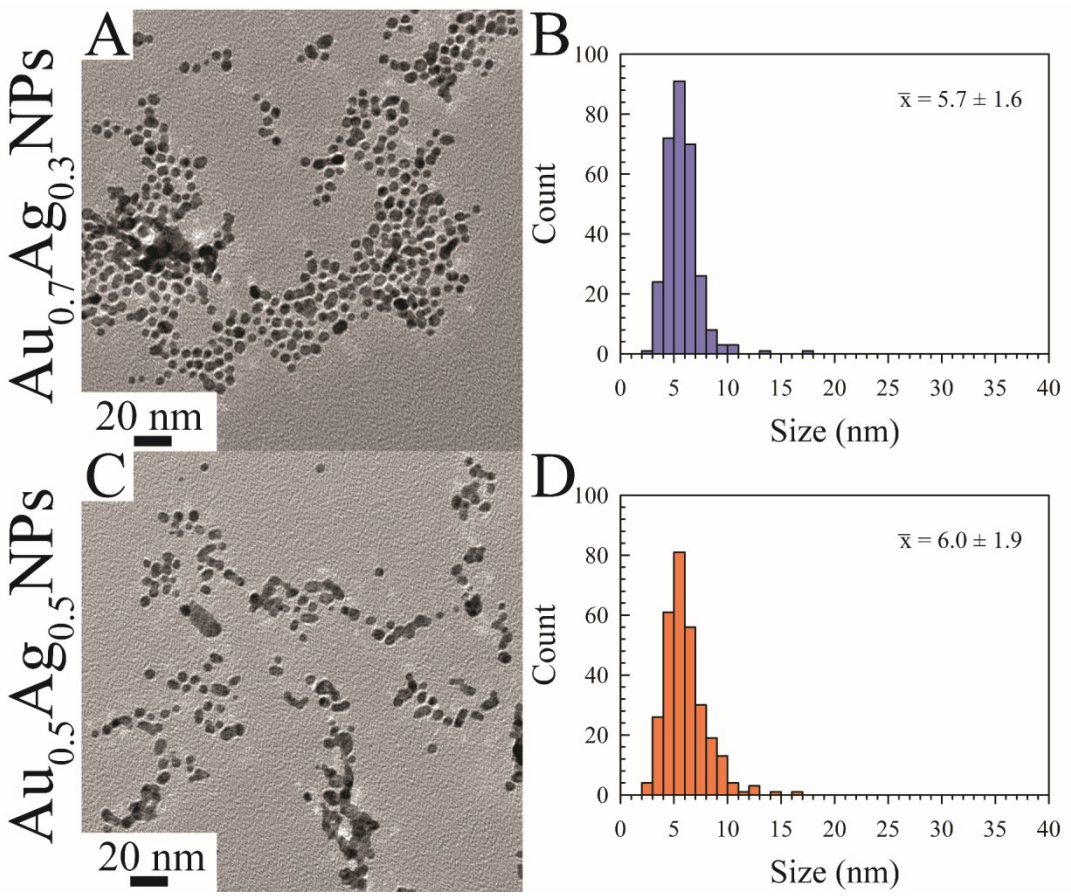

Fig. S15 Representative TEM images and size distribution histograms for R = 10 AuxAg1–xNPs, for (A, B) x = 0.7 and (C, D) x = 0.5. Note the occasional large nanoparticle or aggregation of nanoparticles, particularly in panel C.

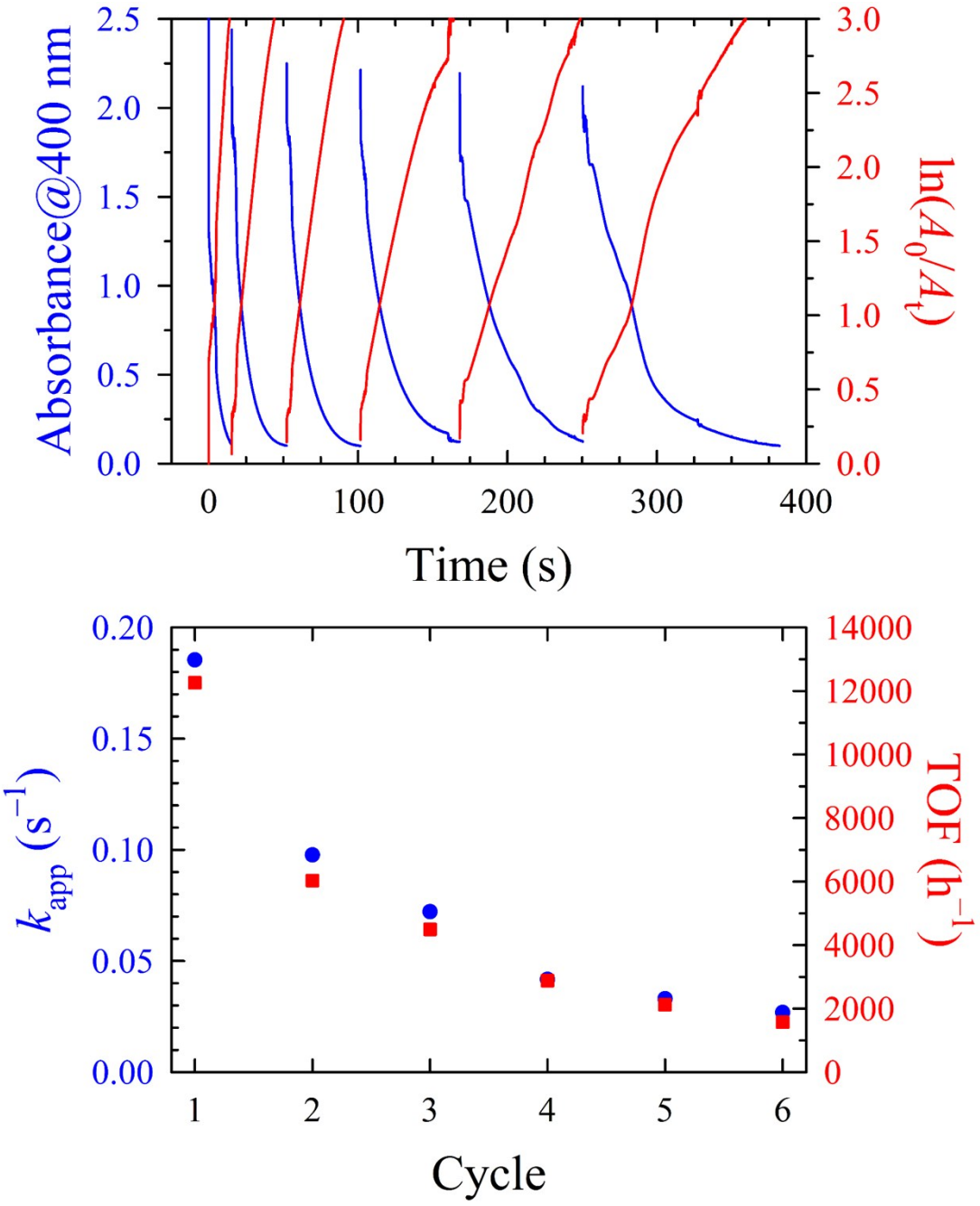

Fig. S16 Assessment of the recyclability of the R = 2, x = 0.3 bimetallic Au_xAg_{1-x}NPs. Top) Absorbance spectra (blue, left axis) and rate plots (red, right axis) for each cycle versus time, with considerable slowing of the reaction rate observed in later cycles. The duration of time between cycles when the cuvette was mixed outside of the instrument has been removed for clarity. Bottom) The k_{app} (blue, left axis) and TOF (red, right axis) values for each cycle, showing exponential decay in activity with sequential cycles.